CHEMISTRY
A EUROPEAN JOURNAL

DOI: 10.1002/chem.200501248

X-ray Diffraction and Theoretical Studies for the Quantitative Assessment of Intermolecular Arene–Perfluoroarene Stacking Interactions

Sergio Bacchi,[a, b] Maurizio Benaglia,[a] Franco Cozzi,[a] Francesco Demartin,[c] Giuseppe Filippini,[d] and Angelo Gavezzotti*[c]

Abstract: The arene–perfluoroarene stacking interaction was studied by experimental and theoretical methods. A series of compounds with different possibilities for formation of this recognition motif in the solid state were synthesized, and their crystal structures determined by single-crystal X-ray diffraction. The crystal packing of these compounds, as well as the packing of related compounds retrieved from crystallographic databases, were analyzed with quantitative crystal potentials: total lattice energies and the cohesive energies of closest molecular pairs in the crystals were calculated. The arene–perfluoroarene recognition motif emerges as a dominant interaction in the non-hydrogen-bonding compounds studied here, to the point that asymmetric dimers formed over the stacking motif carry over to asymmetric units made of two molecules in the crystal both for pure compounds and for molecular complexes; however, inter-ring distances and angles range from 3.70 to 4.85 Å and from 5 to 21°, respectively. Pixel energy partitioning reveals that whenever aromatic rings stack, the largest cohesive energy contribution comes from dispersion, which roughly amounts to 20 kJ mol^{-1} per phenyl ring, while the coulombic term is minor but significant enough to make a difference between the arene–arene or perfluoroarene–perfluoroarene interactions on the one hand, and arene–perfluoroarene interactions on the other, whereby the latter are favored by about 10 kJ mol^{-1} per phenyl ring. No evidence of special interaction which can be attributed to H···F confrontation was recognizable.

Keywords: crystal engineering · molecular recognition · pixel calculations · stacking interactions

Introduction

After the discovery by Patrick and Prosser in 1960 that benzene and hexafluorobenzene form a 1:1 molecular complex,[1] many investigations have been devoted to the geometric and energetic features of the interaction between these two molecules.[2] Structure analysis has demonstrated[3] that in the solid state the benzene and hexafluorobenzene molecules form infinite columns of alternating hydrogenated and fluorinated rings. It was later realized that a parallel stacked structure is widespread among the arene–perfluoroarene complexes, consistent with a simplified model in which the interaction is favored by electrostatic attraction when the charge distributions are approximated by central quadrupoles of opposite phase.[4–6] The discovery of analogous structural motifs in a number of crystallographic studies[7] showed that such alternating columnar arrangements are invariably adopted whenever perfluorinated and hydrogenated aromatic rings are present, either in crystals of pure compounds or of molecular complexes formed by any kind of planar aromatic molecules. The arene–perfluoroarene face-to-face stacking interaction[8] thus emerges as an ubiquitous noncovalent interaction[9,10] that deserves the status of a reliable and robust "synthon" which can be classified and exploited as a structural driving force in supramolecular chemistry and crystal engineering.[11,12]

[a] Dr. S. Bacchi, Dr. M. Benaglia, Prof. F. Cozzi
Dipartimento di Chimica Organica e Industriale
Università degli Studi di Milano
via Venezian 21, 20133 Milano (Italy)

[b] Dr. S. Bacchi
GlaxoSmithKline - Research Center
via Fleming 4, 35131 Verona (Italy)

[c] Prof. F. Demartin, Prof. A. Gavezzotti
Dipartimento di Chimica Strutturale e Stereochimica Inorganica
Università degli Studi di Milano
via Venezian 21, 20133 Milano (Italy)
Fax: (+39) 02-5031-4454
E-mail: angelo.gavezzotti@unimi.it

[d] Dr. G. Filippini
ISTM-CNR, c/o Dipartimento di Chimica Fisica ed Elettrochimica
Università degli Studi di Milano
via Golgi 19, 20133 Milano (Italy)

Supporting information for this article is available on the WWW under http://www.chemeurj.org/ or from the author.

WILEY InterScience DISCOVER SOMETHING GREAT
© 2006 Wiley-VCH Verlag GmbH & Co. KGaA, Weinheim

The crystallographic studies reported so far[3,7,9] have dealt almost exclusively with cocrystals of aromatic hydrocarbons and perfluorohydrocarbons having C–C triple and double bonds but no other functional groups. To the best of our knowledge, only very few studies have presented a detailed description of arene–perfluoroarene interaction in cocrystals of functionalized aromatic molecules. In one of these,[13] it was shown that phenol and pentafluorophenol form columnar face-to-face stacks, and this arrangement was interpreted as mainly due to aryl–perfluoroaryl interactions, which were considered more important than hydrogen-bond formation in determining the structure of the cocrystal. Another study[14] described the solid-state structures of three *N*-pentafluorophenyl benzamides having a nitro, a hydrogen, and a dimethylamino substituent in the *para* position of the benzoyl moiety. In all of the crystal structures, the molecules are linked by infinite H-bonded chains; a face-to-face stacked arrangement between aromatic moieties was observed only in the case of *N*-pentafluorophenyl 4-dimethylaminobenzamide, in which the electron-poor perfluoroaryl residue of one molecule can interact favorably with the electron-rich dimethylaminophenyl residue of another molecule, in agreement with the above-mentioned interpretation of the arene–perfluoroarene interaction in terms of central multipoles.

With a view to a better understanding and a wider practical application of the arene–perfluoroarene interaction as structural determinant in supramolecular chemistry and crystal engineering, it would be highly desirable to acquire more systematic information 1) on the crystal packing of flexible molecular systems without classical hydrogen-bonding functional groups; 2) on the packing modes of molecules carrying both an aromatic and a perfluoroaromatic residue, and thus possibly able to undergo also an intramolecular stacking interaction; and 3) on the competition between the aromatic interaction and other packing forces, such as classical hydrogen bonding, the other prime driving force in crystal packing,[15] and other less energetic recognition patterns. We start here by determining the packing arrangement of molecules whose structure can offer, in the solid state, a choice of interactions among arene–arene, fluoroarene–arene, and fluoroarene–fluoroarene rings: the phenyl and pentafluorophenyl esters of benzene-1,2-dicarboxylic acid and tetrafluorobenzene-1,2-dicarboxylic acid (Scheme 1). The molecules are composed of a "carrier" ring (the phthalic or perfluorophthalic acid ring) and two hydrogenated or fluorinated "prongs". The two prongs have torsional freedom with respect to the carrier ring, but the overall constitution of the molecule allows neither complete ring coplanarity nor intramolecular ring stacking. Henceforth, the mnemonic symbols **H-HH**, **H-FF**, **H-HF**, and **F-HH** will be used for compounds **1**, **2**, **3**, **4** respectively, to indicate the hydrogenated or fluorinated nature of the carrier and the two prongs in that order.

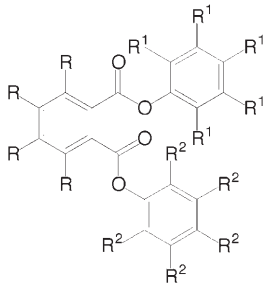

	R	R^1	R^2
1 (**H,HH**)	H	H	H
2 (**H,FF**)	H	F	F
3 (**H,HF**)	H	H	F
4 (**F,HH**)	F	H	H

Scheme 1.

Computational and Theoretical Methods

Qualitative analyses of crystal packing use geometrical criteria for the assessment of the relative importance of energetic factors, and as such, are often affected by subjective judgment. For the quantitative analysis of crystal packing, we use either overall lattice energies, or the concept of neighbor molecular pairs, also called structure determinants:[16] a reference molecule in a crystal structure is picked (the choice is arbitrary), and each molecular pair formed by the reference and one surrounding molecule is characterized by the distance between centers of mass, the symmetry operator connecting the two molecules, and the molecule–molecule interaction energy. In the simplest approach, intermolecular energies are computed by atom–atom potentials supplemented by a separately optimized F···F interaction function;[17] C···F and H···F interaction curves were obtained by the usual averaging procedures. The whole parameter set is collected in Table 1. This formulation is especially attractive because it gives the complete lattice energy without recourse to any separate coulombic sums and thus does not require the derivation of atomic charge parameters. This advantage is obtained at the price of poor selectivity among structures with small differences in coulombic energy. Point-charge coulombic energies were separately calculated by summations over atomic charge parameters obtained from the electrostatic potential fit procedure ("pop = ESP" command) embedded in the Gaussian program suite.[18]

Table 1. UNI force-field parameters[17] for atom–atom energy in the form $E = A\exp(-BR) - CR^{-6}$, with distances R in Å and energies in kJ mol^{-1}. No coulombic R^{-1} terms need be added. $R°$ is the minimum-energy distance, and ε the well depth in kJ mol^{-1}.

	A	B	C	$R°$	ε
H–F	64257.8	4.110	248.36	3.29	−0.110
F–F	170916.4	4.220	564.84	3.20	−0.293
H–H	24158.4	4.010	109.20	3.36	−0.042
C–C	226145.2	3.470	2418.35	3.89	−0.387
H–C	120792.1	4.100	472.79	3.29	−0.205
C–F	196600.9	3.840	1168.75	3.50	−0.350

A more reliable evaluation of intermolecular interaction energies is obtained by the Pixel method.[19] In this approach, the molecular electron density is first calculated by standard quantum chemical methods to give a delocalized description of the electron distribution by a large number (ca. 10000) of negative-charge pixels. The coulombic energy is then calculated by sums over pixel–pixel, pixel–nucleus, and nucleus–nucleus coulombic terms. A local polarizability

 © 2006 Wiley-VCH Verlag GmbH & Co. KGaA, Weinheim

is then assigned to each pixel. The electric field generated by pixels and nuclei in surrounding molecules is calculated, and the linear, static polarization energy is evaluated; an empirical damping function, using one disposable parameter, is introduced to avoid singularities. The intermolecular overlap between molecular electron densities is calculated, and the exchange repulsion energy is evaluated as proportional to the overlap integral, with a correction due to the electronegativity differences; the formulation requires two more disposable parameters.[15]

A London-type formula is used to evaluate dispersion energies. The London approach[20] requires an estimate of the "oscillator strength" of the interacting electrons, which is usually approximated by the molecular ionization potential. In the original formulation of the Pixel method, this quantity was taken as the energy of the HOMO, under the assumption that the interacting electrons would be the peripheral ones and hence roughly at the energy level of the HOMO. This assumption works reasonably well with small molecules containing C, H, N, or O atoms, but runs into trouble in heavily fluorinated aromatic compounds, where the interacting electrons belong in fact, at least in good part, to the fluorine atoms, whose ionization potential is much lower than the energy of the HOMO, which is usually a π-type molecular orbital. In an attempt to correct this deficiency, the London oscillator strength L_p was calculated separately for each pair of interacting molecules, taking into account the different nature of the interacting electrons [Eq. (1)],

$$L_p = \sum_{ij}(I_o^i + I_o^j)/2\, S_{ij} \quad (1)$$

where the summation runs on all atomic species in the molecules, I_o^i is a rescaled atomic ionization potential for atomic species i, and S_{ij} the percentage of the total overlap between the charge densities due to species i and j. The rescaled ionization potentials were taken as 0.300, 0.362, and 0.463 hartree for carbon, hydrogen, and fluorine, respectively. The procedure amounts in fact to taking different dispersion-energy coefficients according to the different kinds of approaching atomic basins. The overall performance of this modification was checked by calculating the lattice energy of a few crystals for which the heat of sublimation is known (see Table 2).

The Pixel method has been successfully applied to the calculation of energies of gas-phase dimers, where it has been demonstrated[15] that the quality of the Pixel results is often similar to that of quantum chemical calculations, at a fraction of the computational cost. The Pixel method allows the calculation of lattice energies in good agreement with crystal sublimation enthalpies for a wide selection of organic compounds, and also performs well in energy ranking for polymorphs of organic crystal structures.[21]

Table 2. Aryl–perfluoroaryl crystals: lattice energies and cohesion energies of the molecular stacked dimer (kJ mol^{-1}).

Compound	Molecular complex with	Crystal: CSD refcode[a]	ΔH_{subl}[b]	$-E$(lattice)		$-E$(dimer)[c]	
				UNI	Pixel	UNI	Pixel
perfluoronaphthalene	–	OFNAPH01	79*	81	73	-	
perfluorobiphenyl	–	DECFDP01	86*	92	81	-	
4,4′-difluorobiphenyl	–	ZZZAOS02	91*	93	98	-	
hexafluorobenzene	–	computer-generated[d]	49*	54	43		
1,2,3,4,5-pentafluorobiphenyl	–	PFBIPH	81	93	97	41	36
1-phenyl-2-perfluorophenylacetylene	–	ASIJIW	92	101	101	48	45
1-phenyl-2-perfluorophenylethylene	–	SERQEL	100	110		51	
hexafluorobenzene	benzene	BICVUE01	90	99		18	20
	naphthalene	IVOBOK	118	124		28	
	pyrene	ZZZGKE01	145	162		38	
	anthracene	ZZZGMW01	143	146		32	
	trans-stilbene	TIJTUB	145	153		21	
perfluoronaphthalene	biphenyl	ASAKIO	154	173		39	
	anthracene	ECUTUR	171	177		46	
	pyrene	ECUVIH	173	189		52	
	triphenylene	ECUVON	187	207		55	
	naphthalene	NPOFNP	146	157		36	47
	diphenylacetylene	OCAYIA	165	174		38	
	acenaphthene	XUNJAR	158	173		42	
perfluorobiphenyl	biphenyl	BPPFBP	162	180		44	52
	naphthalene	CEKYUM	154	161		27	30
perfluorotriphenylene	triphenylene	CUKXIP	228	259		75	
perfluorodiphenylacetylene	diphenylacetylene	ASIJER	184	199		47	46

[a] CSD: see reference [23]. Table S1 (Supporting Information) contains full literature references. [b] Values with asterisk: experimental heats of sublimation; other values: sum of the sublimation enthalpies of the corresponding hydrocarbons (benzene 45, naphthalene 73, anthracene 98, pyrene 100, stilbene 100, biphenyl 81, triphenylene 114, diphenylacetylene 92, acenaphthene 85 kJ mol^{-1}). All data from reference [24]. [c] For one-component crystals, stacking energy of the parallel dimer showing aryl–perfluoroaryl interaction; for binary crystals, stacking energy of the complex dimer. Unoptimized geometries as found in the crystal. [d] The experimental crystal structure of hexafluorobenzene is rather poor; a computer-generated monoclinic polymorph with one molecule in the asymmetric unit was used instead.

 © 2006 Wiley-VCH Verlag GmbH & Co. KGaA, Weinheim

Quantum mechanical molecular energies and electron densities were calculated by Gaussian[18] at the MP2/6-31G** level. All molecular geometries were fixed as extracted from the corresponding crystal structures, except for the usual renormalization of C–H geometries with a C–H distance of 1.08 Å. The lattice energies were calculated by including in the crystal model all molecules up to a separation between molecular centers of 18 Å. All crystal-packing calculations were carried out using the OPiX program package,[22] which includes a packing analysis and atom–atom lattice energy calculation module (ZipOpec), a polymorph generation module including a lattice energy minimizer (Prom-Minop modules), and a module for the calculation of the dimer and lattice energies by the Pixel method.

The Cambridge Structural Database[23] was searched for crystal structures of compounds which could undergo aryl–perfluoroaryl interactions, and the NIST database[24] was searched for thermodynamic functions of aromatic hydrocarbons and aromatic fluorinated compounds. The results are collected in Table 2.

Results and Discussion

Single-crystal X-ray diffraction of **1**–**4** reveals that all intramolecular bond lengths and angles are within normal ranges: C–F distances are 1.332–1.340 Å in **H-HF** and **F-HH**, and range from 1.32 to 1.35 Å in **H-FF**. Molecules in the crystal (Figure S1, Supporting Information) exhibit a wide range of conformational flexibility. Inter-ring angles have been calculated as the angle ($<90°$) formed by the unit vectors along the direction of maximum inertia of the ring formed by the six carbon atoms. They are (carrier–prong 1, carrier–prong 2, prong 1–prong 2, respectively): 42, 30, and 57° in **H-HH**; 21, 55, and 57° in **H-HF**; 60, 65, and 70° in **H-FF**, molecule A; 20, 87 and 88 in **H-FF**, molecule B; and 5, 75 and 72° in **F-HH**. These angles thus span the full range between coplanar and orthogonal, and are different even in the two molecules in the asymmetric unit of **H-FF**. This is clear evidence that molecular conformation in the crystal is driven by intermolecular forces.

There are practically no short atom–atom contacts involving fluorine atoms: just one H···F distance of 2.41 Å (sum of atomic radii 2.56 Å),[25] and one C···F distance of 2.95 Å (sum of atomic radii 3.23 Å), both in **H-FF**. We thus see no need for a discussion of special atom–atom bonding interactions involving fluorine.[10] Other short atom–atom contacts involve the ester groups: O···H (sum of average atomic radii 2.68 Å): 2.34, 2.41, and 2.45 Å in **H-FF**; 2.46 Å in **H-HH**; and 2.52 Å in **H-HF**; C···O (sum of atomic radii 3.35 Å): 3.13 Å in **H-FF** and a strikingly short 3.09 Å in **F-HH**. Discussing short contacts in terms of atom–atom bonding hardly seems advisable; inasmuch as a short contact implies a bond, then one should also discuss an incipient intermolecular F–C···O=C bond in the last-named cases above.

For comparison, the Cambridge Database was searched for characteristic arene–perfluoroarene stacking patterns. Figures S2 and S3 (Supporting Information) show an impressive gallery of packing diagrams for the crystal structures in Table 2 in which the parallel-stacked interaction motif between an aryl and a perfluoroaryl moiety appears. This motif is ubiquitous for any kind of aromatic pair. For an assessment of the implied energies, we first calculated the interaction energies of isolated benzene–benzene, benzene–hexafluorobenzene, and hexafluorobenzene–hexafluorobenzene dimers (Table 3). Complete fluorination brings about a 20% stabilization with respect to the hydrocarbon; mixed interaction doubles the dimerization energy. While the bulk of stabilization comes from dispersion, as is easily predictable in aromatic systems with polarizable π-electrons, the energy difference between homodimers and the heterodimer is entirely due to the coulombic-polarization term. In view of these results, it is not correct to state that the arene–perfluoroarene dimerization energy is essentially coulombic; rather, the coulombic component makes the difference in stabilization.

Table 3. Pixel results for the binding energies [kJ mol^{-1}] of parallel stacked dimers at an inter-ring distance of 3.6 Å.

Compound	E_{coul}[a]	E_{pol}[b]	E_{disp}[c]	E_{rep}[d]	E_{tot}[e]
C_6H_6–C_6F_6	−7.5	−2.2	−22.2	11.7	−20.2
C_6F_6–C_6F_6	2.7	−2.1	−22.4	10.7	−11.2
C_6H_6–C_6H_6	2.7	−2.1	−22.0	12.9	−8.5

[a] Pixel coulombic energy. [b] Pixel polarization energy. [c] Pixel dispersion energy. [d] Pixel repulsion energy. [e] Total Pixel energy for the molecular pair.

The UNI force field arene–perfluoroarene stacking energies (Table 2) are strikingly similar to those obtained by much more sophisticated methods; however, this is probably due to a cancellation of errors, since the UNI force field overestimates the aromatic stacking energy and misses the extra coulombic stabilization in the heterodimer. The arene–perfluoroarene energy advantage appears clearly from the data in Table 2: on average, the lattice energies of mixed compounds are 10–20% larger than the sum of the sublimation enthalpies of the corresponding hydrocarbons. The dimerization energies are additive over the number of rings: for example, benzene–hexafluorobenzene 18, naphthalene–perfluoronaphthalene 36, triphenylene–perfluorotriphenylene 75 kJ mol^{-1}; for the same perfluorinated moiety, the dimerization energy increases smoothly with increasing number of rings in the hydrogenated partner.

The Pixel partitioned lattice energies are listed in Table 4 along with the atom–atom energies. The Pixel method cannot be applied to the **H-FF** crystal, because of a technical problem with two molecules in the asymmetric unit. Pixel and UNI total lattice energies agree in the relative ranking. In the crystals of these aromatic compounds, the dispersion contributions mostly come from interactions between the electron densities of the aromatic ring, and the most effective arrangement is a parallel-stack structure. Stabilizing coulombic interactions may come from contacts be-

 © 2006 Wiley-VCH Verlag GmbH & Co. KGaA, Weinheim

Table 4. Pixel partitioned lattice energies [kJ mol^{-1}].

Compound	E_{coul}[a]	E_{qq}[b]	E_{pol}[c]	E_{disp}[d]	E_{rep}[e]	E_{tot}[f]	E_{UNI}[g]
H-HH	−48	−24	−18	−179	87	−157	−161
H-HF	−38	−18	−15	−170	70	−153	−158
H-FF	–	–	–	–	–	–	−158
F-HH	−32	−16	−13	−155	63	−137	−149

[a] Pixel coulombic energy. [b] Coulombic energy estimated by the point-charge method. [c] Pixel polarization energy. [d] Pixel dispersion energy. [e] Pixel repulsion energy. [f] Total Pixel lattice energy. [g] Lattice energy estimated by the UNI atom–atom force field.[17]

tween positively charged rims and negatively charged cores of the benzene rings in a T-shaped arrangement, or from contact between positively charged aromatic hydrogen regions and negatively charged oxygen regions at the ester linkage, mostly at or around the carbonyl oxygen atoms (what is usually denoted briefly as C−H···O interactions). Destabilizing coulombic interactions are expected between parallel-stacked benzene rings, while stabilizing coulombic interactions are expected between benzene and fluorobenzene moieties. In fact, both the **H-HH** and the **H-HF** crystal structures are largely built on dispersive interactions. However, the **H-HH** crystal has a larger coulombic component, perhaps contrary to expectation: the reason is that, being unable to take advantage of aryl–perfluoroaryl interactions, this structure relies more heavily on stabilizing contact between C−H···O interactions (see below). Interactions between C−H hydrogen atoms and the benzene π clouds are significantly present only in the **F-HH** crystal. Taken together, these results outline a broad ranking of packing effects in these crystals, as aryl–perfluoroaryl > C−H···O coulombic > C−H···π.

The **F-HH** crystal structure (cell volume 433 Å per molecule) is less densely packed than the **H-HF** structure (cell volume slightly smaller, 424 Å per molecule, in spite of having one fluorine atom more than **F-HH**): this is clearly reflected in the smaller lattice energy of **F-HH**, as calculated by both UNI and Pixel; the latter calculation reveals a substantial loss in dispersion energy. The reasons for this must be somehow related to differences in electron density of CF_5 and $CF_4(COO)_2$ rings.

In the **H-HH** crystal (Table 5 and Figure 1) the most stabilizing structural pair (A) also has the largest coulombic

Table 5. Interacting pairs (structure determinants) in the **H-HH** crystal (see Figure 1).

Symmetry operator[a]	E_{coul}[b]	E_{pol}[c]	E_{disp}[d]	E_{rep}[e]	E_{Pixel}[f]	E_{UNI}[g]
A (I; 0, 1, 1)	−21	−8	−46	26	−49	−40
B (I; −1, 1, 1)	−19	−6	−36	16	−45	−36
C (I; 0, 0, 1)	−13	−4	−40	23	−35	−38
D (I; −1, 0, 1)	−9	−3	−31	14	−30	−31
E (G; 0, 1/2, ±1/2)	−8	−4	−27	14	−25	−27

[a] Symmetry labels: I, inversion center; G, glide plane. [b] Pixel coulombic energy. [c] Pixel polarization energy. [d] Pixel dispersion energy. [e] Pixel repulsion energy. [f] Total Pixel energy for the molecular pair. [g] Energy of the molecular pair estimated by the UNI atom–atom force field.[17] Energies in kJ mol^{-1}.

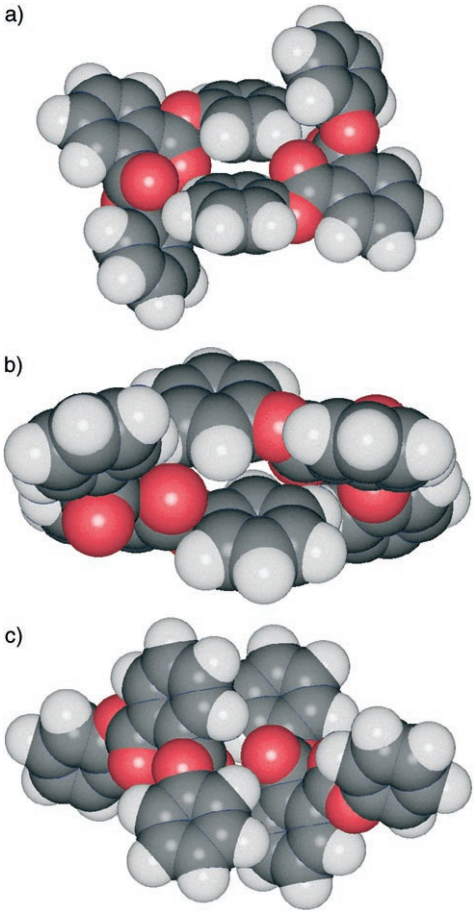

Figure 1. The **H-HH** crystal structure: molecular dimers A, B, and C (a to c).

and dispersion contributions. This pair shows efficient interlocking of the aromatic rings, in which the two prongs of one molecule embrace one prong in the other, but without arene stacking; at the same time, one of the prongs is able to form a favorable contact with the oxygen-rich region of the carrier, with a short C=O···H−C distance of 2.46 Å. The second pair (B) shows a contact between an almost parallel arrangement of the carrier and one prong in the two molecules, and the second prong is turned away from contact. This arrangement provides another source of substantial coulombic stabilizing interaction, with O···H distances of around 2.6 Å; the dispersion contribution is smaller, due to smaller ring overlap, but the repulsion is also smaller, for the same reason, and the two effects balance out. The third pair (C) shows a significant decrease in coulombic stabilization and a resisting amount of dispersion stabilization, in compliance with a more parallel stack-type arrangement. The next pair (D) is essentially a stacking of the two carrier rings, with a small coulombic contribution and a still significant dispersion contribution. While the first pairs have inversion-center symmetry, the next three pairs consist of ribbons along glide plane or screw axes. Consistent with the complex shape of the molecule, these string symmetries are less effective in crystal stabilization.

 © 2006 Wiley-VCH Verlag GmbH & Co. KGaA, Weinheim

Contrary to the crystal structure of **H-HH**, which shows almost a continuum of cohesive energies of the molecular pairs, the crystal structure of **H-HF** (Table 6) shows a largely

Table 6. Interacting pairs (structure determinants) in the **H-HF** and **F-HH** crystals (see Figures 2–4).

Symmetry operator[a]	E_{coul}	E_{pol}	E_{disp}	E_{rep}	$E_{tot,Pixel}$	$E_{tot,UNI}$
H-HF						
A (T; 0, 1, 0)	−8	−4	−58	20	−50	−61
B (S; 0, ±1/2, 1/2))	−13	−5	−28	19	−27	−23
C (G; 0, −1/2, ±1/2)	−7	−3	−24	10	−25	−23
D (I; 1, 0, 1)	−2	−1	−28	8	−24	−23
F-HH						
A (I; 1,1,0)	−12	−5	−75	35	−57	−74
B (I; 1,1,1)	−10	−3	−29	10	−32	−28
C (I; 0,0,0)	−13	−4	−24	14	−28	−23

[a] Symmetry labels: I, inversion center; G, glide plane; S, screw axis; T, identity. See footnotes to Table 5 for other symbols.

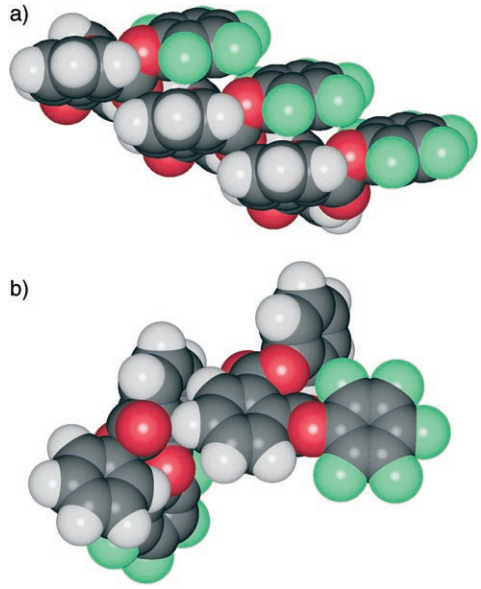

Figure 2. The **H-HF** crystal: molecular dimers A (a) and B (b).

predominant pair (A, Figure 2) whose cohesive energy is more than twice that of any other pair. This pair is clearly formed over a strongly predominant energetic driving force, that is, the simultaneous stacking of offset arene and arene–perfluoroarene rings, easily obtained by pure translation. The nature of this interaction is almost completely dispersive, and coulombic terms contribute very little. The C–H···O-type interactions appear only in the second best pair (B, Figure 2), with a herringbone structure reaching a moderate coulombic stabilization at the expense of a large decrease in dispersion stabilization. The C pair has another arene–perfluoroarene stacking mode, while further pairs (Figure 3) are less interpretable, good examples of what may be called "anonymous" structural pairs, which contribute in a substantial way to the crystal stabilization but have

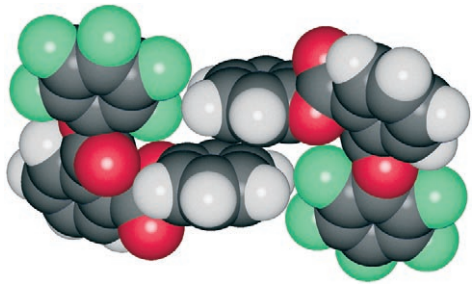

Figure 3. **H-HF** crystal: molecular pair D.

no special features in terms of structure and hence are less attractive to the chemist's eye. The result is that these important pairs are often neglected in cursory crystal-packing analyses based only on short atom–atom distances or other conspicuous structural features.

The **F-HH** structure determinants (Table 6) are somewhat similar in energy and configuration to those of the **H-HF** crystal: an arene–perfluoroarene stacking interaction again dominates the packing (Figure 4), while the second best recognition mode is a double perpendicular arene–arene motif, classifiable as a C–H···π interaction, although the coulombic

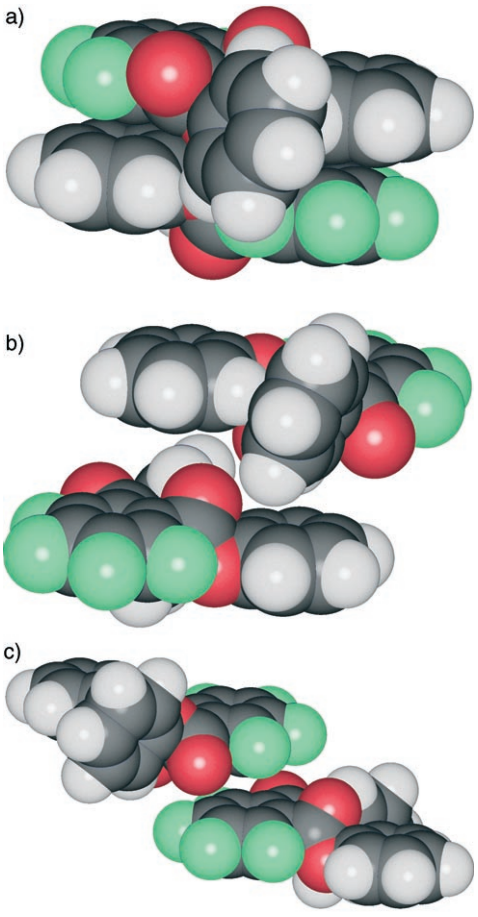

Figure 4. The **F-HH** crystal: molecular pairs A, B, and C (a to c).

 © 2006 Wiley-VCH Verlag GmbH & Co. KGaA, Weinheim

contribution is not particularly large. The third determinant shown in Figure 4 is another example of "anonymous" dimer: if a particular motif is to be recognized at all, it would be a sort of incipient "nucleophilic attack" of a carbonyl oxygen atom on a fluorine-carrying, positively charged carbon atom (very short F–C···C=O distance of 3.09 Å).

The largely dominant driving force in the packing of the **H-FF** crystal (Table 7) is again an arene–perfluoroarene

Table 7. Interacting pairs (structure determinants) in the **H-FF** crystal (see Figure 5).

Symmetry operator[a]	E_{coul}	E_{pol}	E_{disp}	E_{rep}	E_{Pixel}	E_{UNI}
A (Z; 0, 0, 0)	−14	−5	−51	22	−49	−55
B (Z; α translation, 0, −1, 0)	−13	−4	−31	11	−37	−39
C (I_α; 1, 2, 1)	−6	−4	−40	21	−28	−38
D (T_β; 1, 0, 0)	−7	−4	−34	17	−28	−21
E (Z; α translation, −1, 0, 0)	−1	−2	−33	15	−21	−33

[a] Symmetry labels: Z, symmetry-unrelated α and β molecules in the asymmetric unit; I, inversion center; T, identity. See footnotes to Table 5 for other symbols.

stacking interaction, which is evident in all the highest ranking molecular pairs (Figure 5). So strong is the drive to arene–perfluoroarene interaction that the crystal includes

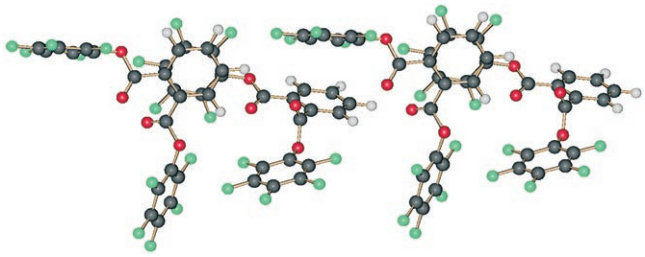

Figure 5. The **H-FF** crystal: molecular pairs A and B. Arene–perfluoroarene stacking occurs in two directions.

two molecules in the asymmetric unit, so that both fluorinated prongs have the possibility to interact with the hydrogenated carrier. Figure 6 shows the impressive structure that results, with columns of stacked single rings and alternating ribbons of fluorinated and hydrogenated rings. Since nearly all cohesive forces in this crystal come from aromatic-ring stacking, the most relevant energy contribution is the dispersion contribution. The smaller coulombic contribution in dimers A and B results from contact between ester oxygen atom and benzene rim (C–H) regions, which involves some short O···H distances of 2.41 (A), 2.54 (B), and 2.45 Å (C). The shortest O···H distance (2.33), in pair F, which is not among the highest ranking in the crystal, confirms that O···H distances are not reliable indicators of cohesive strength.

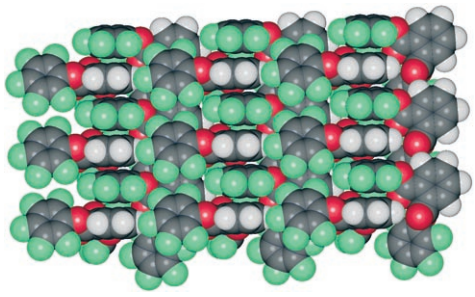

Figure 6. Crystal packing of **H-FF**. Horizontal: *b* translation, vertical: *a* translation. The columns of alternating arene–perfluoroarene rings seen edge-on are clearly visible. The ribbons of perfluoroarene rings sit on top of corresponding ribbons of arene rings. This view is perpendicular to the view in Figure 5.

Conclusion

Our theoretical and experimental analysis quantitatively confirms the qualitative idea that the stacked arene–perfluoroarene recognition pattern is a stable and reproducible one. The crystal structures of isomorphic compounds in which benzene and perfluorobenzene rings alternate show a preference for organization in heterodimers (H···F rings) versus homodimers (H···H or F···F rings). A database study of arene–perfluoroarene molecular complexes reveals that the dimer forms the asymmetric unit in the crystal and invariably has the closest intermolecular contact. Quantitative analysis shows that it is a significant driving force in crystal packing; with a cohesive energy of 20–25 kJ mol^{-1} per phenyl ring, it is second only to hydrogen bonding in carboxylic acids and amides (30–35 kJ mol^{-1} per bond), it competes with weaker hydrogen bonds such as those found in alcohols (25 kJ mol^{-1} per bond), and it largely overcomes all kinds of weaker binding modes commonly invoked in crystal-packing analyses, such as C–H···O hydrogen bonding, which cannot exceed 10 kJ mol^{-1}.[15] This energetic stability does not, however, entail a stringent structural form: the distances between ring centroids in aromatic–perfluoroaromatic contacts and the corresponding inter-ring angles found in the crystal structures of the compounds we have examined are 3.70 (5), 3.95 (6), 4.17 (20), 4.75 (20), and 4.85 Å (21°). The arene–perfluoroarene "synthon" can thus bear a stretch of as much as 1 Å and angular flexion of about 20°.

Calculations of partitioned energies by the Pixel method clearly show that all stacked-arene cohesive interactions are mainly dispersive in nature, and arise from electron correlation between π-electron clouds. However, coulombic energies obviously differ, since those between homodimers are generally repulsive and destabilizing by some 3 kJ mol^{-1}, while that in the heterodimer is stabilizing by about 8 kJ mol^{-1}. Thus, cohesion is mainly generated by dispersion, but structural selectivity depends on coulombic terms.

Our results in terms of Pixel partitioned energies produce a clear quantitative picture of the energetic ranking of molecular recognition modes in organic crystals. While the absolute values may vary by a few kilojoules per mole, in more accurate (e.g., fully ab initio) treatments, the relative orderings do not.[15] Even rough estimates based on empiri-

 © 2006 Wiley-VCH Verlag GmbH & Co. KGaA, Weinheim

cal atom–atom force fields can give acceptable quantitative insights. This analysis further[26,27] shows that when all interacting neighbors in a crystal structure are properly considered with their relative energies, conclusions based on simple analysis of some short distances and preconceived "synthons" are easily overthrown.

Experimental Section

Synthesis: Diphenyl 1,2-benzenedicarboxylate[28] (**1**, **H-HH**) and bis(pentafluorophenyl) 1,2-benzenedicarboxylate[29] (**2**, **H-FF**) were prepared according to literature procedures. They were purified by recrystallization from hexane to afford analytically pure, sharply melting materials (**1**: m.p. 76 °C; lit.:[28] 74–76 °C. **2**: m.p. 96 °C; lit.:[29] 96–97 °C).

Pentafluorophenyl phenyl 1,2-benzenedicarboxylate (3, H-HF): Triethylamine (0.155 mL, 5.41 mmol) and then a solution of pentafluorophenol (0.907 g, 4.92 mmol) in dry THF (2 mL) were added to a stirred solution of phthaloyl dichloride (1.0 g, 4.92 mmol) in dry THF (8 mL). A white precipitate formed. The suspension was stirred at room temperature for 3 h, and the reaction was quenched by addition of saturated aqueous ammonium chloride (15 mL). The organic phase was separated, and the aqueous phase was extracted with dichloromethane (2×15 mL). The combined organic phases were dried over sodium sulfate, filtered, and concentrated under vacuum to afford a yellow oil (1.73 g). The crude product, which was contaminated with about 50 % of phthaloyl dichloride by HPLC analysis, was purified by flash chromatography with cyclohexane:dichloromethane (9:1) as eluant. The obtained product (0.8 g), which was still contaminated with phthaloyl dichloride (ca. 20 % by HPLC), was dissolved in EtOAc and subjected to flash chromatography on a short column with cyclohexane:ethyl acetate (9:1) as eluant. On standing, the obtained colorless oil (0.703 g), which was still contaminated with about 5 % phthaloyl chloride (by HPLC), became a white waxy solid. It was used without further purification. A solution of triethylamine (0.11 mL, 0.784 mmol) and phenol (0.067 g, 0.713 mmol) in dry THF (2 mL) was added to a stirred solution of this product (0.250 g, 0.713 mmol) in dry THF (5 mL). A white precipitate formed. The suspension was stirred at room temperature for 3 h, and the reaction was quenched by addition of saturated aqueous ammonium chloride (15 mL). The organic phase was separated, and the aqueous phase was extracted with ethyl acetate (2×15 mL). The combined organic phases were dried over sodium sulfate, filtered, and concentrated under vacuum to afford a colorless oil (0.281 g). This was purified by flash chromatography with cyclohexane:EtOAc (95:5) as eluant to afford three fractions. The first (0.114 g) was unconverted starting material, which was recycled; the second (0.043 g) was a mixture of starting material and product, which was purified by flash chromatography; and the third fraction (0.025 g) was the product, which was >90 % pure by HPLC. The overall yield of product was 15 % (0.047 g). White needles (m.p. 107.5–108 °C) were obtained from dichloromethane:hexane. IR (Nujol): $\tilde{\nu}$ = 1764.8, 1754.5, 1519.0, 1464.3, 1262.4, 1092.8, 1043.1 cm^{-1}; ^{1}H NMR (400 MHz, $CDCl_3$): δ = 10 (dd, J = 1.2, 7.6 Hz, 1H), 8.03 (dd, J = 1.2, 7.6 Hz, 1H), 7.80 (dt, J = 1.2, 7.6 Hz, 1H), 7.59 (dt, J = 1.2, 7.6 Hz, 1H), 7.45 (t, J = 8.0 Hz, 1H), 7.25–7.32 ppm (m, 3H); ^{13}C NMR (100 MHz, $CDCl_3$): δ = 165.5, 162.7, 150.7 (2 C), 141.3 (J_{C-F} = 251.0 Hz), 141.0 (J_{C-F} = 252.5 Hz), 138.0 (J_{C-F} = 254 Hz), 133.0, 132.8, 131.7, 130.0, 129.8, 129.5, 128.5, 126.2, 121.3 ppm; ^{19}F NMR (376 MHz, $CDCl_3$): δ = −151.7 (d, J = 21.1 Hz, 2F), −157.3 (t, J = 22.6 Hz, 1F), −161.9 ppm (d, J = 19.9 Hz, 2F); elemental analysis (%) calcd for $C_{20}H_9F_5O_4$: C 58.84, H 2.22; found: C 59.48, H 2.05.

Diphenyl 3,4,5,6-tetrafluoro-1,2-benzenedicarboxylate (4, F-HH): A catalytic amount of DMF (1 drop) was added to a stirred solution of tetrafluorophthalic acid (0.5 g, 2.10 mmol) in thionyl chloride (20 mL), and the resulting mixture was refluxed under nitrogen for 18 h. The reaction mixture was then evaporated under vacuum and the crude oil was used as such in the next step. A solution of 4-dimethylaminopyridine (0.10 g, 0.84 mmol) and phenol (0.37 g, 3.73 mmol) in pyridine (1.4 mL) was added to a stirred solution of the dichloride (0.46 g, 1.69 mmol) in dry dichloromethane (5 mL). The yellow solution was stirred under nitrogen for 24 h; the reaction was quenched by addition of water (5 mL), and the resulting mixture was extracted with EtOAc (3×10 mL). The combined organic phases were washed with water (4×10 mL), dried over sodium sulfate, filtered, and concentrated under vacuum to afford a red oil. This was purified by flash chromatography with a cyclohexane:EtOAc (95:5) as eluant to afford the product as a white solid (0.305 g, 0.781 mmol, 46 % yield). This was crystallized from pentane to give large crystals (m.p. 77 °C). IR (Nujol): $\tilde{\nu}$ = 1748.3, 1519.0, 1482.8, 1458.7, 1213.2, 1184.3 cm^{-1}. ^{1}H NMR (400 MHz, [D$_6$]DMSO): δ = 7.51 (t, J = 8.0 Hz, 4H), 7.38 (t, J = 8.0 Hz, 2H), 7.23 (d, J = 7.6 Hz, 4H), 7.59 (dt, J = 1.2, 7.6 Hz, 1H), 7.45 (t, J = 8.0 Hz, 1H), 7.25–7.32 ppm (m, 3H); ^{13}C NMR (100 MHz, [D$_6$]DMSO): δ = 160.5, 150.2, 146.2 (J_{C-F} = 250.0 Hz), 143.0 (J_{C-F} = 252.0 Hz), 130.5, 127.4, 121.6, 116.3 ppm; ^{19}F NMR (376 MHz, [D$_6$]DMSO): δ = −147.4 (d, J = 15.0 Hz, 2F), −136.3 ppm (d, J = 15.0 Hz, 2 F); elemental analysis (%) calcd for $C_{20}H_{10}F_4O_4$: C 61.55, H 2.58; found: C 61.87, H 2.43.

X-ray crystallography: Data were collected at room temperature on a CAD4 diffractometer. No absorption corrections were applied. No intensity decay was detected during data collection. The structures were solved by direct methods (SIR2000)[30] and refined by full-matrix least-squares technique on F^2 (SHELXL-97).[31] Anisotropic thermal parameters were assigned to all non-hydrogen atoms, while hydrogen atoms were placed in calculated positions and refined using a riding model. Crystallographic data are collected in Table 8. Further details: room temperature; least squares on reflections with $I > 2\sigma(I)$; **1**: $C_{20}H_{14}O_4$, M = 318.31, μ = 0.09 mm^{-1}, 1825 reflections and 217 parameters, final $R1$ = 0.045, $wR2$ = 0.147, GOF = 1.074; **2**: $C_{20}H_4O_4F_{10}$, M = 498.23, μ = 0.18 mm^{-1}, 3358 reflections and 613 parameters, final $R1$ = 0.048, $wR2$ = 0.207, GOF = 0.872; **3**: $C_{20}H_9O_4F_5$, M = 408.27, μ = 0.15 mm^{-1}, 1580 reflections and 262 parameters, final $R1$ = 0.058, $wR2$ = 0.118, GOF = 0.994; **4**: $C_{20}H_{10}O_4F_4$, M = 390.28, μ = 0.13 mm^{-1}, 2533 reflections and 253 parameters, final $R1$ = 0.039, $wR2$ = 0.114, GOF = 1.012.

Table 8. Crystal data.[a]

Compound	Space group, Z	a	b	c	α	β	γ	ρ_{exptl} [g cm^{-3}]	V[b] [Å^3]
H-HH	$P2_1/c$, 4	8.884	12.580	14.507	–	98.32	–	1.318	401.1
H-FF	$P\bar{1}$, 4	7.532	12.784	20.287	100.10	97.27	91.40	1.737	476.4
H-HF	$P2_1/c$, 4	18.590	5.975	17.073	–	116.57	–	1.599	424.0
F-HH	$P\bar{1}$, 2	7.709	10.560	11.945	105.09	99.75	106.92	1.497	433.0

[a] Cell edges in angstroms, cell angles in degrees. Typical standard deviations are 0.002 Å for cell edges, and 0.02° for cell angles. [b] Cell volume per mole.

CCDC 285979–285982 contain the supplementary crystallographic data for this paper. These data can be obtained free of charge from the Cambridge Crystallographic Data Centre via www.ccdc.cam.ac.uk/data_request/cif.

Acknowledgements

The pictures were drawn with the help of the program SCHAKAL.[32] Financial support by MIUR (FIRB 2001 grant number RBAU018XA7 to F.C.J. is gratefully acknowledged.

 © 2006 Wiley-VCH Verlag GmbH & Co. KGaA, Weinheim

[1] C. R. Patrick, G. S. Prosser, *Nature* **1960**, *187*, 1021.
[2] For an early review, see: J. H. Williams, *Acc. Chem. Res.* **1993**, *26*, 593–598; for quantum-chemical theoretical calculations on aromatic–fluoroaromatic systems, see: M. O. Sinnokrot, E. F. Valeev, C. D. Sherrill, *J. Am. Chem. Soc.* **2002**, *124*, 10887–10893; P. Hobza, H. L. Selzle, E. W. Schlag, *J. Phys. Chem.* **1996**, *100*, 18790–18794; A. P. West, S. Mecozzi, D. A. Dougherty, *J. Phys. Org. Chem.* **1997**, *10*, 347–350; J. Hernandez-Trujillo, F. Colmenares, G. Cuevas, M. Costas, *Chem. Phys. Lett.* **1997**, *265*, 503–507; Y. Zhao, D. G. Truhlar, *J. Phys. Chem. A J. Phys. Chem. B* **2005**, *109*, 4209–4212; W. B. Schweizer, J. D. Dunitz, *J. Chem. Theor. Comp.* **2005**, *1*, 834–840 and references therein; force-field treatment of aromatic interactions: G. Chessari, C. A. Hunter, C. M. R. Low, M. J. Packer, J. G. Vinter, C. Zonta, *Chem. Eur. J.* **2002**, *8*, 2860–2867. See also ref. [15].
[3] a) J. Vrbancich, G. L. D. Ritchie, *J. Chem. Soc. Faraday Trans. 2* **1980**, 648–659; b) M. Luhmer, K. Bartik, A. Dejaegere, P. Bovy, J. Reisse, *Bull. Soc. Chim. Fr.* **1994**, *131*, 603–606; J. C. Collings, P. S. Smith, D. S. Yufit, A. S. Batsanov, J. A. K. Howard, T. B. Marder, *CrystEngComm* **2004**, *6*, 25–28, and other papers by the same group in Table S1 (see Supporting Information).
[4] For a quantitative evaluation of the effect on arene–arene interaction exerted by increasing fluorine substitution on one of two parallel-stacked aromatic rings, see: F. Cozzi, F. Ponzini, R. Annunziata, M. Cinquini, J. S. Siegel, *Angew. Chem.* **1995**, *107*, 1092–1093; *Angew. Chem. Int. Ed. Engl.* **1995**, *34*, 1019–1020.
[5] a) C. A. Hunter, J. K. M. Sanders, *J. Am. Chem. Soc.* **1990**, *112*, 5525–5534; b) F. Cozzi, M. Cinquini, R. Annunziata, J. S. Siegel, *J. Am. Chem. Soc.* **1993**, *115*, 5330–5331, and references therein; c) F. J. Carver, C. A. Hunter, E. M. Seward, *Chem. Commun.* **1998**, 775–776.
[6] J. H. Williams, J. K. Cockroft, A. N. Fitch, *Angew. Chem.* **1992**, *104*, 1666–1668; *Angew. Chem. Int. Ed. Engl.* **1992**, *31*, 1655–1657.
[7] Review: K. Reichenbächer, H. I. Süss, J. Hulliger, *Chem. Soc. Rev.* **2005**, *34*, 22–30.
[8] For a review on the proteiform aspects of aromatic–aromatic interactions and their implications in many areas of chemistry, see E. A. Meyer, R. K. Castellano, F. Diederich, *Angew. Chem.* **2003**, *115*, 1244–1287; *Angew. Chem. Int. Ed.* **2003**, *42*, 1210–1250.
[9] a) G. W. Coates, A. R. Dunn, L. M. Henling, D. A. Dougherty, R. H. Grubbs, *Angew. Chem.* **1997**, *109*, 290–293; *Angew. Chem. Int. Ed. Engl.* **1997**, *36*, 248–251; b) G. W. Coates, A. R. Dunn, L. M. Henling, J. W. Ziller, E. B. Lobkovsky, R. H. Grubbs, *J. Am. Chem. Soc.* **1998**, *120*, 3641–3649; c) C. Dai, P. Nguyen, T. B. Marder, A. J. Scott, W. Clegg, C. Viney, *Chem. Commun.* **1999**, 2493–2494; d) M. L. Renak, G. P. Bartholomew, S. Wang, P. J. Ricatto, R. J. Lachicotte, G. C. Bazan, *J. Am. Chem. Soc.* **1999**, *121*, 7787–7799; e) F. Ponzini, R. Zagha, K. Hardcastle, J. S. Siegel, *Angew. Chem.* **2000**, *112*, 2413–2415; *Angew. Chem. Int. Ed.* **2000**, *39*, 2323–2325; f) W. J. Feast, P. W. Lövenich, H. Puschmann, C. Taliani, *Chem. Commun.* **2001**, 505–506; g) M. R. Haneline, M. Tsunoda, F. P. Gabbaï, *J. Am. Chem. Soc.* **2002**, *124*, 3737–3742.
[10] The occurrence of a favorable interaction between aromatic H and aromatic F was sometimes suggested as a possible stabilizing factor in these structures (e.g., see refs. [9d] and [9f]). However, it has been noted that organofluorine almost never accepts hydrogen bonds: J. D. Dunitz, R. Taylor, *Chem. Eur. J.* **1997**, *3*, 89–98.
[11] For examples dealing with DNA-like molecules, see: a) K. A. Frey, S. A. Woski, *Chem. Commun.* **2002**, 2206–2207; b) G. Mathis, J. Hunziker, *Angew. Chem.* **2002**, *114*, 3335–3338; *Angew. Chem. Int. Ed.* **2002**, *41*, 3203–3205; c) R. Faraoni, R. K. Castellano, V. Gramlich, F. Diederich, *Chem. Commun.* **2004**, 370–371.
[12] For an example dealing with a catenane molecule, see: R. E. Gillard, J. F. Stoddardt, A. J. P. White, B. J. Williams, D. J. Williams, *J. Org. Chem.* **1996**, *61*, 4504–4505.
[13] S. Meejoo, B. M. Kariuki, K. D. M. Harris, *ChemPhysChem* **2003**, *4*, 766–769.
[14] H. Adams, J.-J. Jimenez Blanco, G. Chessari, C. A. Hunter, C. M. R. Low, J. M. Sanderson, J. G. Vinter, *Chem. Eur. J.* **2001**, *7*, 3494–3503.
[15] The presence of a hydrogen bond can influence a crystal structure so strongly that other, less energetic interactions, such as the arene–perfluoroarene interaction, can be overwhelmed. For an assessment of the relative energies associated with aromatic stacking and with hydrogen-bond formation in crystals, see: A. Gavezzotti, *J. Chem. Theor. Comp.* **2005**, *1*, 834–840, and references therein.
[16] A. Gavezzotti, G. Filippini, *J. Am. Chem. Soc.* **1995**, *117*, 12299–12305.
[17] For the hydrocarbon part, see G. Filippini, A. Gavezzotti, *Acta Crystallogr. Sect. B* **1993**, *49*, 868–880; the F···F interaction-energy curve was optimized essentially by the same procedure, that is, by setting the energy minimum at a distance slightly shorter than the preferred contact distance in crystals of fluorinated compounds, and adjusting the well depth to reproduce a few crystal heats of sublimation (see Table 2).
[18] Gaussian 03, Revision A.1, M. J. Frisch, G. W. Trucks, H. B. Schlegel, G. E. Scuseria, M. A. Robb, J. R. Cheeseman, J. A. Montgomery, Jr., T. Vreven, K. N. Kudin, J. C. Burant, J. M. Millam, S. S. Iyengar, J. Tomasi, V. Barone, B. Mennucci, M. Cossi, G. Scalmani, N. Rega, G. A. Petersson, H. Nakatsuji, M. Hada, M. Ehara, K. Toyota, R. Fukuda, J. Hasegawa, M. Ishida, T. Nakajima, Y. Honda, O. Kitao, H. Nakai, M. Kiene, X. Li, J. E. Knox, H. P. Hratchian, J. B. Cross, C. Adamo, J. Jaramillo, R. Gomperts, R. E. Stratmann, O. Yazyev, A. J. Austin, R. Cammi, C. Pomelli, J. W. Ochterski, P. Y. Ayala, K. Morokuma, G. A. Voth, P. Salvador, J. J. Dannenberg, V. G. Zakrzewski, S. Dapprich, A. D. Daniels, M. C. Strain, O. Farkas, D. K. Malick, A. D. Rabuck, K. Raghavachari, J. B. Foresman, J. V. Ortiz, Q. Cui, A. J. Baboul, S. Clifford, J. Cioslowski, B. B. Stefanov, G. Liu, A. Liashenko, P. Piskorz, I. Komaromi, R. L. Martin, D. J. Fox, T. Keith, M. A. Al-Laham, C. Y. Peng, A. Nanayakkara, M. Challacombe, P. M. W. Gill, B. Johnson, W. Chen, M. W. Wong, C. Gonzalez, J. A. Pople, Gaussian, Inc., Pittsburgh, PA, **2003**.
[19] a) A. Gavezzotti, *J. Phys. Chem.* **2002**, *B106*, 4145–4154; b) A. Gavezzotti, *J. Phys. Chem.* **2003**, *B107*, 2344–2353; c) A. Gavezzotti, *CrystEngComm* **2003**, *5*, 429–438.
[20] F. London, *Trans. Farady Soc.* **1937**, *33*, 8–26.
[21] A. Gavezzotti, *CrystEngComm* **2003**, *5*, 439–446.
[22] A. Gavezzotti, *Z. Kristallogr.* **2005**, *220*, 499–510.
[23] F. H. Allen, O. Kennard, *Chem. Des. Autom. News* **1993**, *8*, 31–37.
[24] H. Y. Afeefy, J. F. Liebman and S. E. Stein, *Neutral Thermochemical Data*; and J. S. Chickos, *Heat of Sublimation Data*, in *NIST Chemistry WebBook*, *NIST Standard Reference Database Number 69* (Eds.: P. J. Linstrom, W. G. Mallard), March **2003**, National Institute of Standards and Technology, Gaithersburg MD, 20899 (http://webbook.nist.gov).
[25] R. S. Rowland, R. Taylor, *J. Phys. Chem.* **1996**, *100*, 7384–7391.
[26] A. Gavezzotti, *Struct. Chem.* **2005**, *16*, 177–185.
[27] J. D. Dunitz, A. Gavezzotti, *Cryst. Growth Des.* **2005**, *5*, 2180–2189.
[28] F. F. Blicke, O. J. Weinkauff, *J. Am. Chem. Soc.* **1932**, *54*, 330–334.
[29] N. Ito, H. Kudo, A. Kameyama, T. Nishikubo, T. Anadia, *J. Polym. Sci. Part A* **2002**, *41*, 213–222.
[30] A. Altomare, M. C. Burla, M. Camalli, G. Cascarano, C. Giacovazzo, A. Guagliardi, A. G. Moliterni, G. Polidori and R. Spagna, *J. Appl. Crystallogr.* **1999**, *32*, 115–119.
[31] G. M. Sheldrick, SHELX-97, University of Goettingen, Germany **1997**.
[32] E. Keller, SCHAKAL92, A Program for the Graphic Representation of Molecular and Crystallographic Models, University of Freiburg, **1993**.

Received: October 10, 2005
Published online: February 28, 2006

 © 2006 Wiley-VCH Verlag GmbH & Co. KGaA, Weinheim